

[CASE REPORT]

Undifferentiated Embryonal Sarcoma of the Liver Identified after the Initial Diagnosis of a Hepatic Cyst

Yusaku Manabe¹, Haruki Uojima¹, Hisashi Hidaka¹, Xue Shao^{1,2}, Shuichiro Iwasaki¹, Naohisa Wada¹, Kousuke Kubota¹, Yoshiaki Tanaka¹, Takahide Nakazawa¹, Akitaka Shibuya¹, Masaaki Ichinoe³, Yusuke Kumamoto⁴, Takashi Kaizu⁴ and Wasaburo Koizumi¹

Abstract:

Abdominal ultrasound in a 50-year-old Japanese man revealed a cystic lesion on the caudate lobe of the liver. Four-month follow-up imaging showed a rapid increase in the size of the cystic lesion. The patient underwent laparoscopic partial hepatectomy because of a suspicion and perceived risk that the lesion might be malignant. The initial histological diagnosis was a hepatic cyst. Eleven months later, computed tomography showed a giant cystic lesion in the abdominal cavity and multiple liver metastases. The patient underwent excision of the giant cystic lesion and a partial hepatectomy. Immunohistochemistry for the recurring lesion revealed undifferentiated embryonal sarcoma of the liver.

Key words: undifferentiated embryonal liver sarcoma, cystic lesion, hydatid cyst

(Intern Med 59: 2375-2382, 2020)

(DOI: 10.2169/internalmedicine.4853-20)

Introduction

Sarcomas of the liver are extremely rare, representing less than 1% of all primary liver tumors (1). Undifferentiated embryonal sarcoma of the liver (UESL) is highly malignant with a poor prognosis. It often occurs in children aged 6-10 years and it tends to be uncommon in adults (2). An early diagnosis of UESL is often difficult because clinical symptoms and imaging findings do not manifest until the later stages of the neoplasm. Therefore, it is essential to recognize characteristic histologic findings and the patterns visualized by immunohistochemical staining to rule out any other types of hepatic lesions (3, 4). We herein report a case of UESL in a 50-year-old man initially diagnosed to be a simple liver cyst.

Case Report

A 50-year-old Japanese man was incidentally found to have a cystic lesion of the liver on abdominal ultrasound (US) when he was examined due to right lower abdominal discomfort. He denied any other symptoms such as weight loss and fever. There was no history of liver disease or drug or food allergies. At the initial physical examination, he appeared well. He had an axillary temperature of 36.0°C, heart rate of 75 beats/minute, blood pressure of 120/60 mmHg, and respiratory rate of 12 breaths/minute. There were no particular abnormal physical findings, including abdominal findings. Laboratory tests revealed no abnormalities, including tumor markers such as alpha-fetoprotein and protein induced by vitamin K absence or antagonist-II (Table). Gadolinium-ethoxybenzyl-diethylenetriamine pentaacetic acid-enhanced magnetic resonance imaging (Gd-EOB-DTPA MRI) demonstrated a cystic lesion measuring 54.6×46.6×

¹Department of Gastroenterology, Internal Medicine, Kitasato University School of Medicine, Japan, ²Department of Hepatopancreatobiliary Medicine, The Second Hospital of Jilin University, China, ³Department of Pathology, Kitasato University School of Medicine, Japan and ⁴Department of Surgery, Kitasato University School of Medicine, Japan

Received: March 13, 2020; Accepted: May 6, 2020; Advance Publication by J-STAGE: June 30, 2020

Correspondence to Dr. Haruki Uojima, kiruha@kitasato-u.ac.jp

Table. Summary of the Laboratory Data.

		Normal range	Previous procedure	after the procedure
Complete blood count				
White blood cells	×10 ² /μL	30-97	41	108
Neutrophils	%	36.6-79.9	62.9	85.3
Haemoglobin	g/dL	13.1-17.6	16.9	14.7
Platelet counts	×10 ⁴ /μL	12.4-30.5	20.2	26.3
Biochemistry				
Total bilirubin	mg/dL	0.1-1.2	0.9	1.2
Aspartate aminotransferase	IU/L	12-35	22	19
Alanine aminotransferase	IU/L	6-40	24	28
Lactate dehydrogenase	IU/L	119-229	173	153
γ-glutamyl transpeptase	IU/L	0-48	19	34
Alkaline phosphatase	IU/L	115-359	153	228
Blood-urea-nitrogen	mg/dL	7.4-19.5	11.1	10.1
Creatinine	mg/dL	0.5-1.2	0.84	0.88
Total protein	g/dL	6.4-8.3	7.1	6.8
Albumin	g/dL	3.8-5.2	4.6	3.4
Sodium	mEq/L	135-147	140	136
Potassium	mEq/L	3.4-4.8	4.5	4.3
Ammonia	μg/dL	12-66	12	
HbA1c	%	4.6-6.2	5.7	5.8
Coagulation				
PT-INR		0.89-1.12	<1.00	1.15
APTT	s	23.6-31.3	25	37.4
Tumor marker				
Alpha-fetoprotein	ng/mL	0-10	6	6
PIVKA-II	mAU/mL	0-39	10	15
Serology				
Hepatitis B surface antigen			Negative	
Hepatitis C virus antibody			Negative	

PT-INR: prothrombin time-international normalized ratio, APTT: activated partial thromboplastin time, PIVKA- II: protein induced by vitamin K absence-II

53.7 mm in size (Fig. 1). The inside of the cystic lesion was not a solid component. The T1 image was homogeneous with a very low signal intensity, and the T2 image showed an increased signal intensity. The clinical diagnosis was a simple liver cyst.

Approximately 4 months later, the patient returned for a follow-up examination.

Gd-EOB-DTPA MRI demonstrated a significant volume increase of the cystic lesion measuring 113×106×112 mm in size (Fig. 2). The inside of the cystic lesion was not solid. The T1 image was homogeneous with a very low signal intensity, and the T2 image showed an increased signal intensity. A partition wall and a film-like structure were recognized around the cystic lesion, but the cyst was not enhanced after the administration of a contrast medium. The patient was asymptomatic; therefore, the diagnosis was uncertain. However, because of a suspicion that the lesion might be malignant, we performed a laparoscopic partial hepatectomy (Fig. 3).

The pathological examination revealed a cellular component in the thickened part of the cyst wall composed of medium-to-large spindle, oval, and stellate cells with marked nuclear pleomorphism. In addition, multinucleated giant

cells and focal periodic acid-Schiff (PAS)-positive cytoplasmic inclusions resistant to diastase digestion were sparsely observed (Fig. 4). These findings were atypical of a simple cyst. To consider a neuromyeloma and solitary fibrosis tumor as a differential diagnosis, we performed immunostaining for CD31, CD34, S-100, and α-SMA. However, all of these were negative.

Based on these findings, the pathological diagnosis was a hepatic cyst.

The procedure was performed without any complications. However, on postoperative day 320, the man was admitted with the chief complaint of epigastric pain. On physical examination, he appeared to be mildly unwell. He had a heart rate of 70 bpm, blood pressure of 120/70 mmHg, body temperature of 38.1°C, and respiratory rate of 12 breaths per minute with an oxygen saturation of 98% on room air. No conjunctival pallor, icterus, cyanosis, or spider nevi were detected. Cardiovascular and respiratory examination indicated normal jugular venous pressure and heart sounds, with no detectable murmurs, and normal breath sounds, with no crackle or wheeze. An abdominal examination revealed spontaneous pain and tenderness of the entire abdomen and a palpable mass in the epigastric region. Laboratory studies

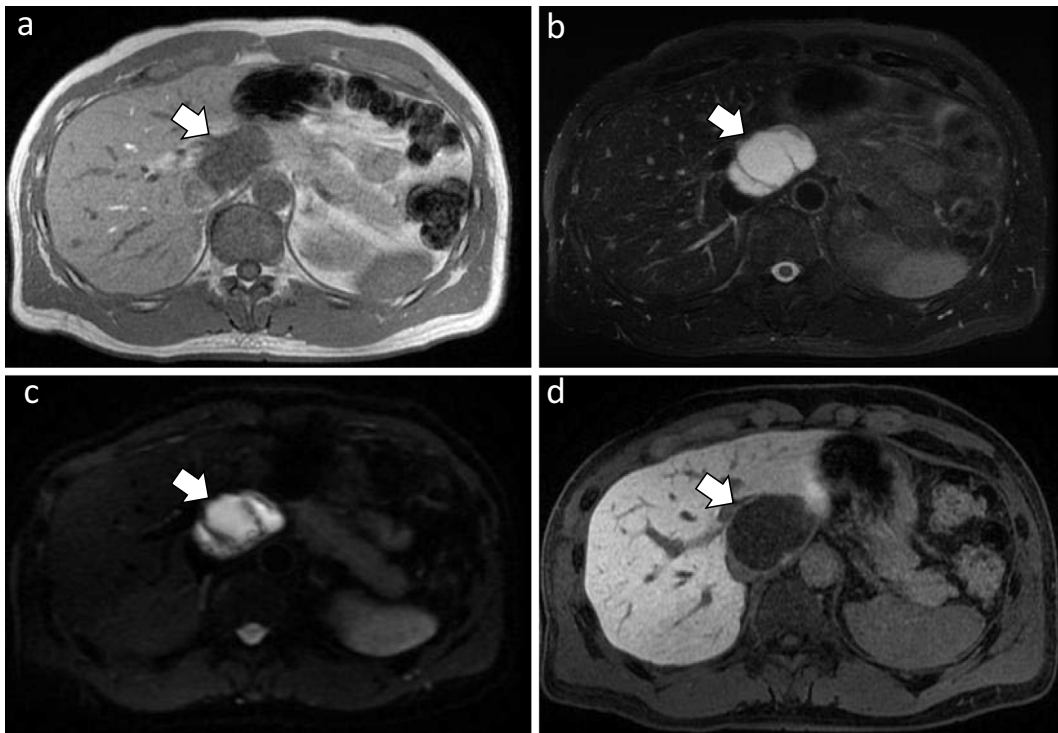


Figure 1. A cystic tumor (54.6×46.6×53.7 mm) (arrow) shows a low intensity on this T1-weighted image (a) and a higher intensity in the T2-weighted image with septums (b). It shows a high intensity in this diffusion-weighted abdominal magnetic resonance image (MRI) (c), and the hepatocellular phase of the ethoxybenzyl (EOB)-MRI showed a low intensity in the cystic tumor (d). a: T1-weighted image, b: T2-weighted image, c: diffusion-weighted image, d: hepatocellular phase.

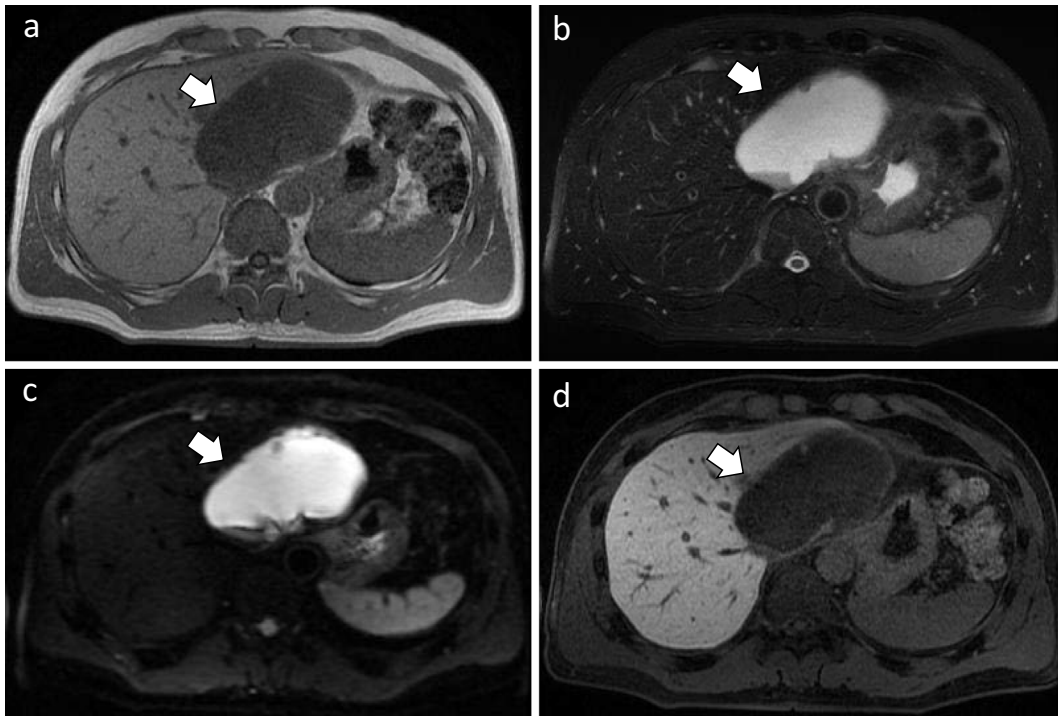


Figure 2. The cystic tumor (113×106×112 mm) (arrow) shows a low intensity on this T1-weighted image (a) and a higher intensity on this T2-weighted image with septums (b). A partition wall and a film-like structure were not enhanced after the administration of contrast medium (d). a: T1-weighted image, b: T2-weighted image, c: diffusion-weighted image, d: hepatocellular phase.

indicated elevated leukocytes, neutrophils, and C-reactive protein, while liver tests and tumor markers were normal (Table). CT showed a giant multilocular cystic lesion in the abdominal cavity and multiple liver metastases. The tumor was located on the posterior side of the stomach and the ventral side of the pancreas, most of which had a cystic appearance, and the inside was suspected of hemorrhaging (Fig. 5). The patient underwent excision of the giant cystic lesion and partial hepatectomy of S4 (Fig. 6).

Pathologically, the tumor had a cystic morphology with a



Figure 3. The resected cystic lesion measured 135×110×3.8 mm in size and was part of a cyst with wall thickening.

septum and an internal hematoma component. The cellular component was composed of medium-to-large spindled, oval, and stellate cells with marked nuclear pleomorphism. Multinucleated giant cells with intracytoplasmic hyaline globules were sparsely observed and were PAS-positive and diastase resistant (Fig. 7). In addition, vimentin, alpha-1-antitrypsin (α 1-AT), and alpha-1-antichymotrypsin (α 1-ACT) were positive (Fig. 8).

These findings were consistent with the diagnosis of UESL. Because the structures of the large cystic lesion in the abdominal cavity were similar to those of the cyst removed in the patient's previous surgery, we also performed immunohistochemical staining. As a result, vimentin, α 1-AT, and α 1-ACT were also positive (Fig. 9). The final diagnosis was a UESL and multiple metastases in the liver.

After the partial hepatectomy, the UESL was considered for treatment with adriacin which is a first-line drug, but the patient received transcatheter arterial chemoembolization (TACE) with epirubicin because the lesion was localized in the liver. After two TACE treatments, CT showed metastatic tumors in the abdominal cavity, and the patient received chemotherapy with eribulin (1.39 mg/m² intravenously). However, after one course, CT showed increased intraperitoneal and liver metastases and the disease progressed significantly, and his general condition gradually worsened. The patient died on postoperative day 729.

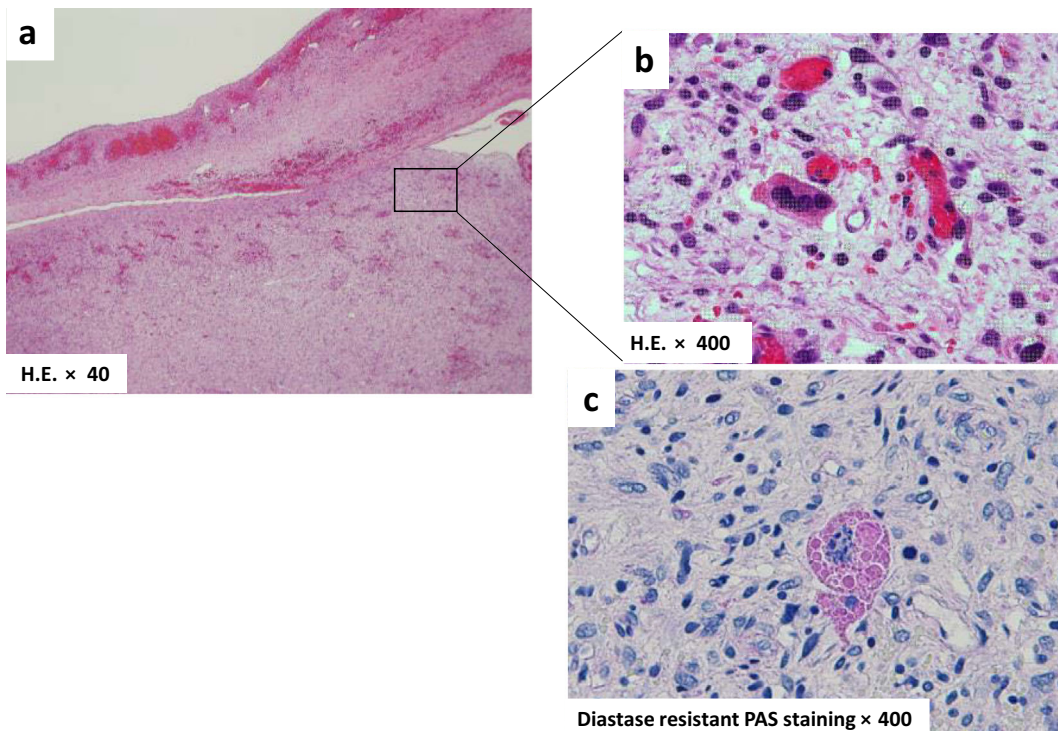


Figure 4. (a) A part of the cyst wall is thickened and had hemorrhagic changes. (b) The cell density is high, and fibrous cells with large and small spindle cells are growing diffusely. (c) The multinucleated giant cells and focal periodic acid-Schiff (PAS)-positive cytoplasmic inclusions resistant to diastase digestion are rarely observed. a: Hematoxylin and Eosin (H&E) staining ×40, b: H&E staining ×400, c: diastase resistant PAS staining ×400.

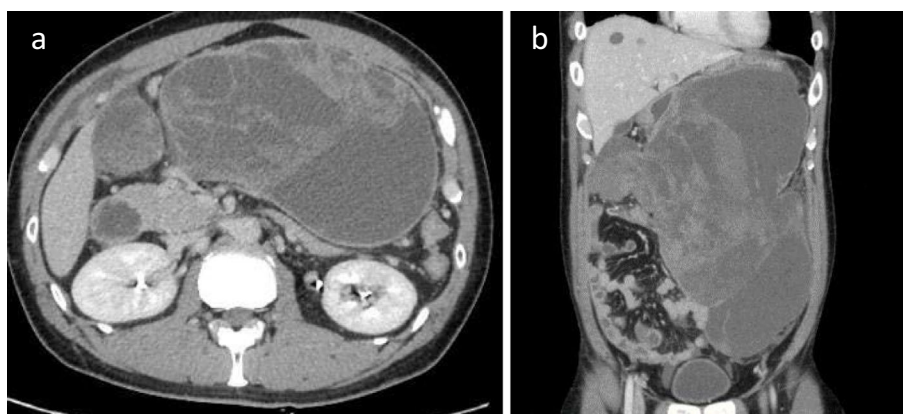


Figure 5. a: Enhanced CT arterial phase. b: The tumor was located on the posterior side of the stomach and on the ventral side of the pancreas, most of which had a cystic appearance, and bleeding was suspected inside the tumor.

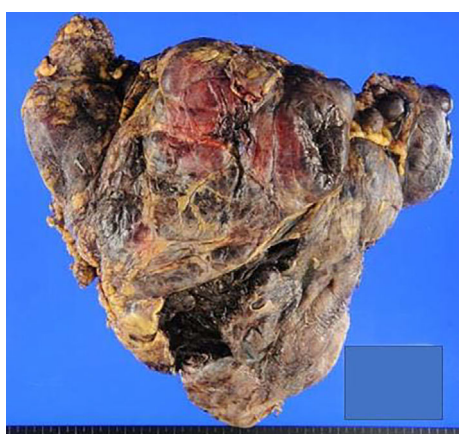


Figure 6. The resected giant cystic tumor measured 24×22.5×7 cm in size, with the morphology of a cyst with a septum, with an internal hematoma component.

Discussion

We report a case of a UESL in a 50-year-old man who was first diagnosed to have a simple liver cyst. UESL is a highly malignant tumor with a poor prognosis, often occurring in children aged 6-10 years, but it is uncommon in adults (2). Stocker and Ishak first proposed the concept and name of UESL in 1978 (5). Between 1977 and 2015, there were 46 reports of adult UESL (6). A recent report summarizing UESL patients had a median age of 25 years, the oldest being a patient 86 years old (7). UESL patients usually present with a variety of symptoms, including anorexia, lethargy, abdominal mass, and abdominal pain associated with weight loss; however, in most cases, the symptoms associated with the tumor are nonspecific. The most common chief complaints of patients with a UESL are abdominal pain or an abdominal mass (4).

In clinical tests, transaminases and tumor markers are usually normal. With hemorrhage and necrosis within the tumor, elevated levels of systemic inflammatory markers, such

as fever, C-reactive protein, erythrocyte sedimentation rate, and leukocytosis, may be present (8). Imaging tests often show a singular or multiple nodular masses in the liver. However, they are nonspecific; and the results of imaging, such as CT, US, and MRI, are often inconclusive (9). US usually shows a large mass with solid and cystic components, which could be mistaken for an abscess or an echinococcal cyst. CT reveals a heterogeneous, multilocular mass with low-density components and an abnormal uptake of contrast medium (8). MRI reveals well-enclosed, low-density multilocular lesions with multiple ultrahigh-density septa and water attenuation. Solid lesions often show an enhanced contrast, but in cases of central necrosis and bleeding, mild and heterogeneous peripheral enhancement may be observed. The interior of the cystic lesion is a liquid component, and MRI shows a low signal intensity on T1-weighted images and high signal intensity on T2-weighted images. Furthermore, the area of hemorrhaging is recognized as a region with a high signal intensity on T1-weighted images and a low signal intensity on T2-weighted images (10).

The pathological features and carcinogenic mechanisms of UESL remain unclear. UESL is basically a single fibrous pseudocystic lesion, surrounded by a gray-white gelatinous cystic component, a solid component and compressed liver parenchyma (12). Microscopically, the cellular component is composed of round, oval, and/or spindle-shaped astrocytes, cells with prominent nuclear polymorphism, and obscure cellular borders in a myxoid matrix.

A peculiar morphological feature occasionally seen is multinucleated giant cells with hyaline spheres in the cytoplasm, which are observed to be PAS-positive and diastase-resistant (4). Immunohistochemistry is generally required to reach a definitive diagnosis and rule out other possible mimickers; however, the staining pattern of UESL is variable and nonspecific. UESL is usually diffusely positive for vimentin and α 1-AT. In addition, UESL may be locally positive for cytokeratin, desmin, α -SMA (alpha-smooth muscle actin), muscle-specific actin, CD68, myoglobin, neuron-specific enolase, α 1-ACT, and S100. In addition, it

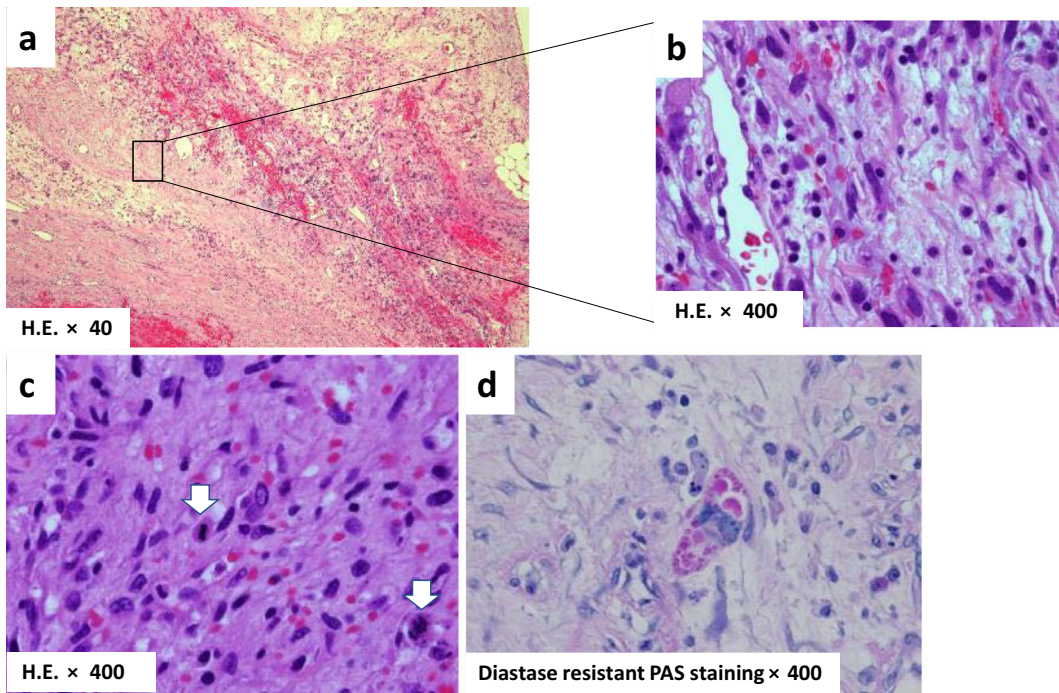


Figure 7. (a) The tumor has a cystic form with a septum and an internal hematoma component. (b) The cellular component is composed of medium-to-large spindled or stellate cells with marked nuclear pleomorphism. (c) In some cases, cells with fission are observed (arrows). (d) The multinucleated giant cells with intracytoplasmic hyaline globules are sparsely observed and are periodic acid-Schiff (PAS)-positive and diastase resistant. a: Hematoxylin and Eosin (H&E) staining $\times 40$, b: H&E staining $\times 400$, c: H&E staining $\times 400$, d: diastase resistant PAS staining $\times 400$.

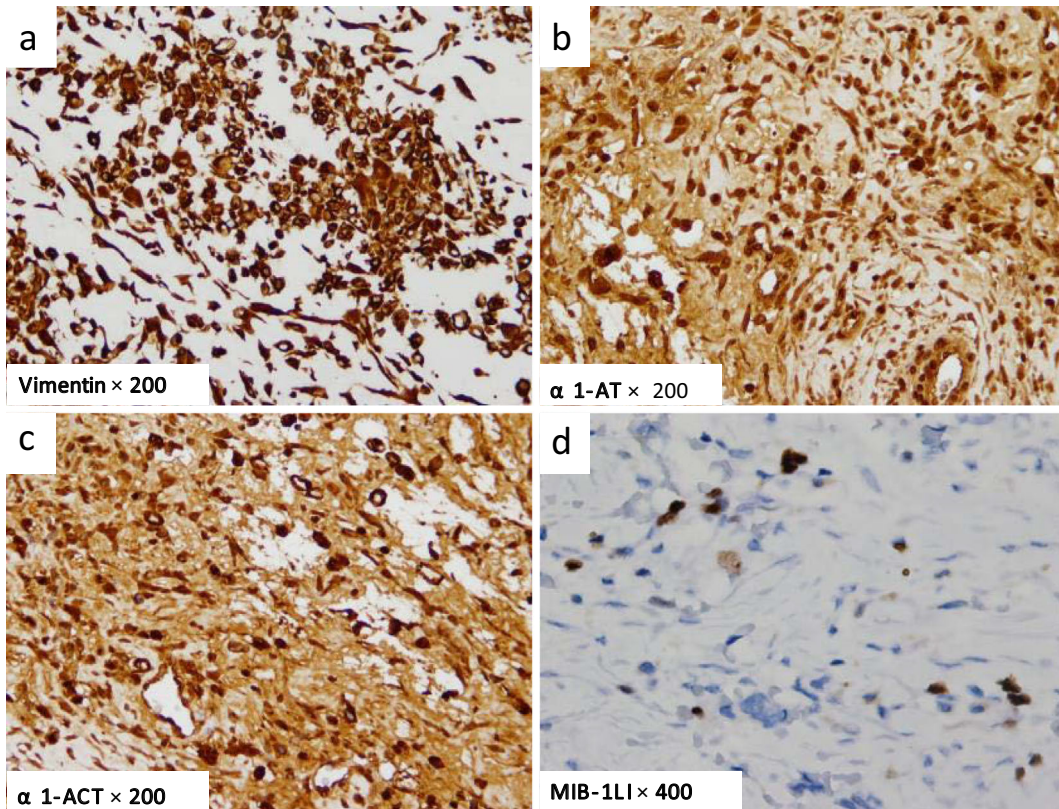


Figure 8. There is positivity for vimentin, alpha-1-antitrypsin ($\alpha 1$ -AT), and alpha-1-antitrypsin ($\alpha 1$ -ACT) in the specimen from the second resection. a: vimentin $\times 200$, b: $\alpha 1$ -AT $\times 200$, c: $\alpha 1$ -ACT $\times 200$, d: MIB-1LI $\times 400$.

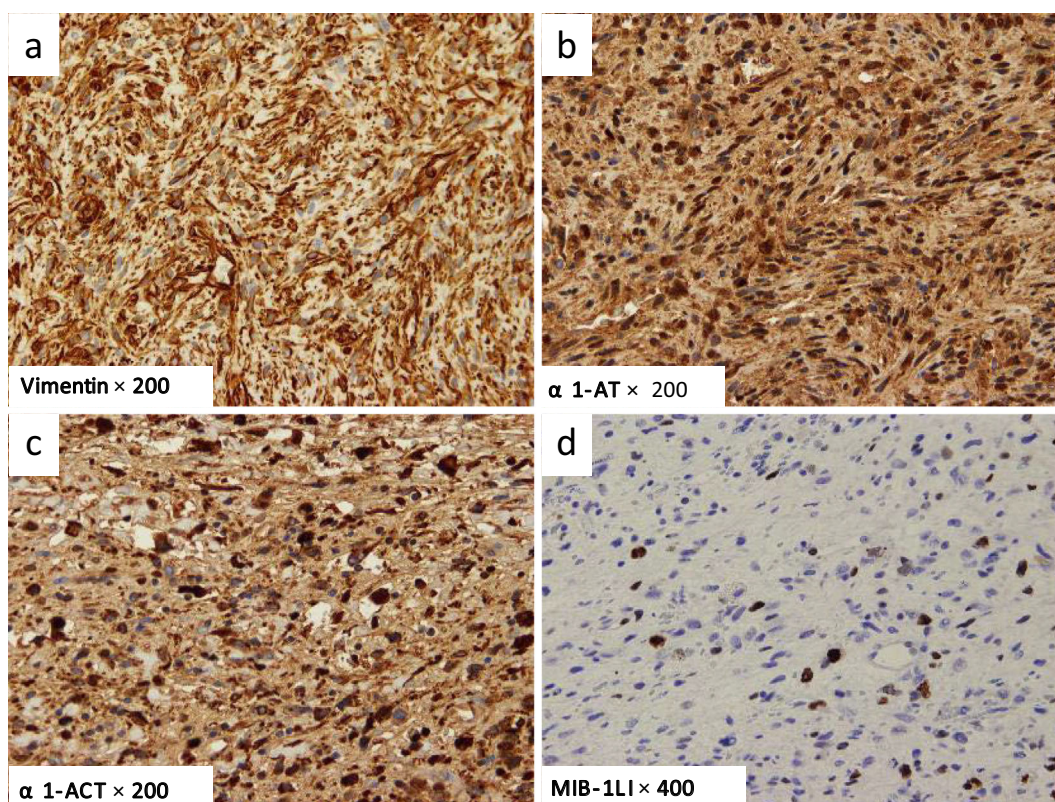


Figure 9. There is positivity for vimentin, alpha-1-antitrypsin (α 1-AT), and alpha-1-antitrypsin (α 1-ACT) in the specimen from the first resection. a: vimentin \times 200, b: α 1-AT \times 200, c: α 1-ACT \times 200, d: MIB-1LI \times 400.

is undifferentiated thus suggesting an embryonal entity (13-15).

This clinical case of UESL was initially diagnosed as a simple liver cyst. Two main points are noteworthy. First, we should consider UESL in the differential diagnosis if the patient had a cystic lesion that rapidly increases in size and then develops a septum and a capsule within a short period of time. In fact, if the physician would have mentioned UESL in the differential diagnosis, then the pathologist might have confirmed the diagnosis of UESL from the first specimen of the resected liver tissue. The patient underwent laparoscopic partial hepatectomy, and pathologically, hematoxylin and eosin staining showed the cellular components consisted of medium-to-large spindle, oval, and stellate cells with nuclear polymorphism. Furthermore, multinucleated giant cells and focal PAS-positive cytoplasmic inclusions resistant to diastase digestion were also observed. These findings were atypical for a simple cyst but were typical for UESL. However, at that time, a clinical diagnosis of a simple liver cyst by the physician made the diagnosis by the pathologist more difficult. As a result, the atypia was not severe but thought to consist of inflammatory or fibrotic changes due to hemorrhaging, and the first histological diagnosis was a misdiagnosis of a complicated hepatic cyst. Second, appropriate immunohistochemical staining should be added for cystic lesions. For atypical findings for a simple cyst, we considered a neuromyeloma and solitary fibrosis tumor in the differential diagnosis. Therefore, we performed

immunostaining for CD31, CD34, S-100, and α -SMA. However, only 11 months after the initial diagnosis, CT showed a multilocular mass with low-density components as the typical image of UESL. A pathological examination of this novel cystic lesion revealed multinucleated giant cells with hyaline spheres that were PAS-positive cytoplasmic inclusions resistant to diastase digestion. The immunohistochemistry results were diffusely positive for vimentin and α 1-AT. Because these findings suggested UESL, we added immunohistochemical staining after the first diagnosis of a hepatic cyst. As a result, vimentin, α 1-AT, and α 1-ACT were also positive. The final diagnosis was UESL and multiple metastases in the liver.

Conclusion

We herein reported a case of UESL in a 50-year-old man whose cystic lesion was initially diagnosed to be a hepatic cyst. If cystic lesions have atypical imaging or pathological findings, then additional immunostaining may help in the diagnosis of UESL.

The authors state that they have no Conflict of Interest (COI).

Acknowledgement

We thank Robert E. Brandt, founder, CEO, and CME, of MedEd Japan, for editing and formatting the manuscript.

References

1. Liver Cancer Study Group of Japan. Primary liver cancer in Japan. Clinicopathologic features and results of surgical treatment. *Ann Surg* **211**: 277-287, 1990.
2. Beksac K, Mammadov R, Ciftci T, Guner G, Akyol A, Kaynaroglu V. Undifferentiated embryonal sarcoma of the liver in an adult patient. *Cureus* **10**: e3037, 2018.
3. Techavichit P, Masand PM, Himes RW, et al. Undifferentiated embryonal sarcoma of the liver (UESL): a single-center experience and review of the literature. *J Pediatr Hematol Oncol* **38**: 261-268, 2016.
4. Putra J, Ornvold K. Undifferentiated embryonal sarcoma of the liver: a concise review. *Arch Pathol Lab Med* **139**: 269-273, 2015.
5. Stocker JT, Ishak KG. Undifferentiated (embryonal) sarcoma of the liver: report of 31 cases. *Cancer* **42**: 336-348, 1978.
6. Lee KH, Maratovich MN, Lee KB. Undifferentiated embryonal sarcoma of the liver in an adult patient. *Clin Mol Hepatol* **22**: 292-295, 2016.
7. Lenze F, Birkfellner T, Lenz P, et al. Undifferentiated embryonal sarcoma of the liver in adults. *Cancer* **112**: 2274-2282, 2008.
8. Wei ZG, Tang LF, Chen ZM, Tang HF, Li MJ. Childhood undifferentiated embryonal liver sarcoma: clinical features and immunohistochemistry analysis. *J Pediatr Surg* **43**: 1912-1919, 2008.
9. Noghuchi K, Yokoo H, Nakanishi K, et al. A long-term survival case of adult undifferentiated embryonal sarcoma of liver. *World J Surg Oncol* **10**: 65, 2012.
10. Buetow PC, Buck JL, Pantongrag-Brown L, et al. Undifferentiated (embryonal) sarcoma of the liver: pathologic basis of imaging findings in 28 cases. *Radiology* **203**: 779-783, 1997.
11. Kim KA, Kim KW, Park SH, et al. Unusual mesenchymal liver tumors in adults: radiologic-pathologic correlation. *AJR Am J Roentgenol* **187**: W487-W489, 2006.
12. Lauwers GY, Grant LD, Donnelly WH, et al. Hepatic undifferentiated (embryonal) sarcoma arising in a mesenchymal hamartoma. *Am J Surg Pathol* **21**: 1248-1254, 1997.
13. Tanaka S, Takasawa A, Fukasawa Y, Hasegawa T, Sawada N. An undifferentiated embryonal sarcoma of the liver containing adipophilin-positive vesicles in an adult with massive sinusoidal invasion. *Int J Clin Exp Pathol* **5**: 824-829, 2012.
14. Pachera S, Nishio H, Takahashi Y, et al. Undifferentiated embryonal sarcoma of the liver: case report and literature survey. *J Hepatobiliary Pancreat Surg* **15**: 536-544, 2008.
15. Kiani B, Ferrell LD, Qualman S, Frankel WL. Immunohistochemical analysis of embryonal sarcoma of the liver. *Appl Immunohistochem Mol Morphol* **14**: 193-197, 2006.

The Internal Medicine is an Open Access journal distributed under the Creative Commons Attribution-NonCommercial-NoDerivatives 4.0 International License. To view the details of this license, please visit (<https://creativecommons.org/licenses/by-nc-nd/4.0/>).